

Online Research @ Cardiff

This is an Open Access document downloaded from ORCA, Cardiff University's institutional repository: <https://orca.cardiff.ac.uk/id/eprint/123682/>

This is the author's version of a work that was submitted to / accepted for publication.

Citation for final published version:

Gwynne, Lauren, Sedgwick, Adam C., Gardiner, Jordan E., Williams, George T., Kim, Gyoungmi, Lowe, John P., Maillard, Jean-Yves ORCID: <https://orcid.org/0000-0002-8617-9288>, Jenkins, A. Toby A., Bull, Steven D., Sessler, Jonathan L., Yoon, Juyoung and James, Tony D. 2019. Long wavelength TCF-based fluorescent probe for the detection of alkaline phosphatase in live cells. *Frontiers in Chemistry* 7 , -. 10.3389/fchem.2019.00255 file

Publishers page: <http://dx.doi.org/10.3389/fchem.2019.00255>
<<http://dx.doi.org/10.3389/fchem.2019.00255>>

Please note:

Changes made as a result of publishing processes such as copy-editing, formatting and page numbers may not be reflected in this version. For the definitive version of this publication, please refer to the published source. You are advised to consult the publisher's version if you wish to cite this paper.

This version is being made available in accordance with publisher policies.

See

<http://orca.cf.ac.uk/policies.html> for usage policies. Copyright and moral rights for publications made available in ORCA are retained by the copyright holders.



Long wavelength TCF-based fluorescence probe for the detection of Alkaline Phosphatase in live cells

Lauren Gwynne¹, Adam C. Sedgwick², Jordan E. Gardiner¹, George T. Williams¹, Gyoungmi Kim³, Jean-Yves Maillard⁴, Toby Jenkins^{1*}, Steven D. Bull^{1*}, Jonathan L. Sessler^{2*}, Juyoung Yoon^{3*}, Tony D. James^{1*}

¹University of Bath, United Kingdom, ²University of Texas at Austin, United States, ³Ewha Womans University, South Korea, ⁴Cardiff University, United Kingdom

Submitted to Journal:

Frontiers in Chemistry

Specialty Section:

Supramolecular Chemistry

Article type:

Original Research Article

Manuscript ID:

446203

Received on:

02 Jan 2019

Revised on:

17 Feb 2019

Frontiers website link:

www.frontiersin.org

Long wavelength TCF-based fluorescent probe for the detection of Alkaline Phosphatase in live cells

Lauren Gwynne¹, Adam C. Sedgwick², Jordan E. Gardiner¹, George T. Williams¹, Gyoungmi Kim³, John P. Lowe¹, Jean-Yves Maillard⁴, A. Toby A. Jenkins^{1*}, Steven D. Bull^{1*}, Jonathan L. Sessler^{2*}, Juyoung Yoon^{3*} and Tony D. James^{1*}

¹Department of Chemistry, University of Bath, Bath, UK.

²Department of Chemistry, University of Texas at Austin, Austin, USA.

³Department of Chemistry and Nano Science, Ewha Womans University, Seoul, Korea.

⁴Cardiff School of Pharmacy and Pharmaceutical Sciences, Cardiff University, Cardiff, UK.

* Correspondence:

Tony D. James, Juyoung Yoon, Jonathan L. Sessler, Steven D. Bull, A. Toby A. Jenkins
T.D.James@bath.ac.uk, jyoon@ewha.ac.k, sessler@cm.utexas.edu, S.D.Bull@bath.ac.uk,
A.T.A.Jenkins@bath.ac.uk

Keywords: Reaction-based fluorescent probe¹, Alkaline Phosphatase², Cell Imaging³

Abstract

A long wavelength TCF-based fluorescent probe (**TCF-ALP**) was developed for the detection of alkaline phosphatase (ALP). ALP-mediated hydrolysis of the phosphate group of **TCF-ALP** resulted in a significant fluorescence ‘turn on’ (58-fold), which was accompanied by a colorimetric response from yellow to purple. **TCF-ALP** was cell-permeable, which allowed it to be used to image ALP in HeLa cells. Upon addition of bone morphogenic protein 2, **TCF-ALP** proved capable of imaging endogenously stimulated ALP in myogenic murine C2C12 cells. Overall, TCF-ALP offers promise as an effective fluorescent/colorimetric probe for evaluating phosphatase activity in clinical assays or live cell systems.

1 Introduction

Alkaline phosphatase (ALP) is an ubiquitous enzyme found in the majority of human tissues, where it catalyses the dephosphorylation of various substrates such as nucleic acids, proteins and other small molecules (Millán, 2006, Coleman, 1992). ALP also plays an important role in signal transduction and regulation of intracellular processes (cell growth, apoptosis and signal transduction pathways) (Julien et al., 2011). Abnormal levels of ALP in serum are an indicator of several diseases including bone disease (Garnero and Delmas, 1993), liver dysfunction (Rosen et al., 2016), breast and prostatic cancer (Ritzke et al., 1998, Wymenga et al., 2001) and diabetes (Tibi et al., 1988). As a result, ALP is regarded as a key biomarker in medical diagnosis (Coleman, 1992, Ooi et al., 2007). Therefore, it is important to develop a fast, reliable and selective detection system for monitoring ALP activity that is amenable to clinical diagnostics.

There have been numerous approaches to determine ALP levels, including colorimetric (Yang et al., 2016, Hu et al., 2017), chemiluminescent (Jiang and Wang, 2012), electrochemical (Zhang et al., 2015b), surface-enhanced Raman methods (Ruan et al., 2006) and fluorescence (Cao et al., 2016, Fan

et al., 2016). This work focused on the development of fluorescent probes for the detection of biologically relevant analytes (Sedgwick et al., 2017a, Sedgwick et al., 2018b, Wu et al., 2017, Sedgwick et al., 2017b, Sedgwick et al., 2018a, Zhang et al., 2019). Fluorescence has many advantages over other methods owing to its simplicity and high sensitivity/selectivity, providing rapid, non-invasive, real-time detection (Wu et al., 2017). Whilst there have been many fluorophores developed for assaying ALP activity such as organic dyes (Zhang et al., 2015a, Zhao et al., 2017), conjugated polymers (Li et al., 2014), inorganic semiconductor dots (Qian et al., 2015), and noble metal clusters (Sun et al., 2014), most require high probe concentrations and crucially rely on short wavelength emission, thus limiting their applicability in biological systems. Therefore, ALP probes that operate at long wavelengths are urgently required. Such probes should allow for deeper tissue penetration and be subjected to less cell-based autofluorescence (Liu et al., 2017, Zhang et al., 2017, Tan et al., 2017).

2 Results and Discussion

2.1 Chemistry

Here we report a TCF-based fluorescent probe that allows for the detection of ALP and/or ACP. As shown in **Scheme 1**, this probe (**TCF-ALP**) is based on the conjugation of 2-dicyanomethylene-3-cyano-4,5,5-trimethyl-2,5-dihydrofuran (**TCF**) to an electron-donating moiety, a phosphorylated phenol; this affords an internal charge transfer (ICT) donor- π -acceptor (D- π -A) system whose fluorescence properties vary dramatically following ALP-mediated phosphate group cleavage (Gopalan et al., 2004, Liao et al., 2006, Lord et al., 2008, Bouffard et al., 2008, Jin et al., 2010, Teng et al., 2018, Sedgwick et al., 2017b). **TCF-ALP** was synthesised in four steps with an overall yield of 27% (**Scheme 2**). In brief, 3-hydroxy-3-methyl-2-butanone, malononitrile and NaOEt were heated at reflux in EtOH for 1 h. The resultant precipitate **TCF** (**1**) was then treated with a mixture of piperidine (cat.) and 4-hydroxybenzaldehyde in EtOH to afford intermediate **2** (**TCF-OH**). Intermediate **2** was then treated with diethylchlorophosphate, DMAP (cat.) and NEt_3 in THF to give the phosphonate ester **3**. Hydrolysis using trimethylsilyl iodide in dichloromethane (DCM) afforded **TCF-ALP** as a crystalline solid (Et_2O).

2.2 Spectroscopic studies of TCF-ALP

UV-Vis and fluorescence spectroscopic titrations of **TCF-ALP** were performed in 50 mM Tris-HCl buffer in the absence and presence of ALP from porcine kidney. In the absence of ALP, **TCF-ALP** was found to have no UV absorption features above ~ 550 nm; however, upon addition of ALP a bathochromic shift in the UV absorption maximum was observed (from 440 to 580 nm), which was accompanied by a change in colour from yellow to purple (**Figure S1**). ALP-mediated hydrolysis of **TCF-ALP** to form highly fluorescent phenol (**2**), was confirmed by ^{31}P NMR studies and HRMS (See **Figure S1 – S4**). The effect of pH on the rate of ALP mediated hydrolysis of **TCF-ALP** was evaluated. It was found that incubation with 0.8 U/mL of ALP at pH 9.2 resulted in the largest fluorescence response (**Figure S5**). Consequently, all *in vitro* experiments to determine ALP activity were carried out in 50 mM Tris-HCl buffer at pH 9.2.

The kinetics of ALP towards **TCF-ALP** were determined *via* fluorescence spectroscopy (**Figure S6 and S7**), with the resultant fluorescence data analysed using the Michaelis-Menten equation (**Figure S8**). This revealed a K_m of 35.81 ± 2.63 μM and a V_{max} of 3029 ± 157.3 min^{-1} for hydrolysis of **TCF-ALP** by ALP at pH 9.2 (see SI for details). **TCF-ALP** was then incubated with various concentrations of ALP (0.0 – 0.2 U/mL) for 15 minutes to evaluate its ability to monitor ALP activity. As shown in **Figure 1**, a significant fluorescence response was observed in the presence of ALP (58-fold) with a limit of detection (LOD) calculated as 0.12 mU/mL (**Figure S9**). This sensitivity is comparable to other

fluorescent probes found in literature (**Table S3**). Although serum alkaline phosphatase levels vary with age in normal individuals (Lowe et al., 2018), it is widely accepted that serum ALP levels in healthy adults lies between 39 – 117 U/mL (Sahran et al., 2018, Saif et al., 2005). This suggests that **TCF-ALP** is capable of detecting ALP in human serum, and therefore could be used in clinical assays.

Inhibition studies were carried out in the presence of sodium orthovanadate (Na_3VO_4), which is known to be a strong inhibitor of ALP activity. Addition of Na_3VO_4 resulted in a decrease in the fluorescence response in the **TCF-ALP** hydrolysis assay (see **Figure S10**) (Swarup et al., 1982). These inhibition studies enabled an IC_{50} of 6.23 μM to be calculated (**Figure S11**), which is similar in value to other ALP substrates that have been reported in the literature (Tan et al., 2017, Zhang et al., 2015a).

The selectivity of **TCF-ALP** towards other biologically relevant enzymes (at their optimal pH values) was then determined (**Figure 2** and **S12**), with **TCF-ALP** displaying high substrate selectivity for ALP over other common hydrolytic enzymes (e.g. trypsin, porcine liver esterase) or non-specific binding proteins (e.g. bovine serum albumin (BSA)). Interestingly, **TCF-ALP** produced a fluorescence response when treated with acid phosphatase (ACP). The detection of this enzyme is of significance since it is a tumour biomarker for metastatic prostate cancer (Makarov et al., 2009). Normal levels of ACP in serum range from 3.0 – 4.7 U/mL, and elevated ACP levels can be indicative of a variety of other diseases (Bull et al., 2002). Furthermore, **TCF-ALP** proved capable of detecting ACP (25-fold fluorescence enhancement) and ALP (38-fold enhancement) at a physiological pH of 7.1 (**Figure S13** and **S14**). Kinetic determination of ALP and ACP towards **TCF-ALP** at pH 7.1 was conducted, and the resultant K_m and V_{\max} were compared (see **SI 2.1** and **Figures S15-S18**). It was found that ALP has a smaller K_m value in comparison to ACP ($0.38 \pm 0.042 \mu\text{M}$ and $99.22 \pm 13.16 \mu\text{M}$ respectively) and a lower V_{\max} ($208 \pm 3.81 \text{ min}^{-1}$ and $1962 \pm 223.6 \text{ min}^{-1}$ respectively). Hence, ALP has higher affinity towards **TCF-ALP** compared to ACP, thus is more selective towards ALP at physiological pH.

According to current standards, determination of ALP and ACP is undertaken at the phosphatase's optimum pH. For example, the Centers for Disease Control and Prevention (CDC) procedure for ALP determination is carried out in 2-amino-2-methyl-1-propanol (AMP) buffer at pH 10.3 ((CDC), 2012). This is in accordance with other literature sources (Guo et al., 2018, Di Lorenzo et al., 1991, Radio et al., 2006, Pandurangan and Kim, 2015). Likewise, ACP determination is carried out at pH 4-6 (Myers and Widlanski, 1993, Boivin and Galand, 1986, LI et al., 1984). Following these observations, further studies were conducted to determine selectivity at pH 5.0 and 9.2 (**Figures S19 – S22**). Results showed that **TCF-ALP** acts selectivity towards ACP at acidic pH, and ALP at alkaline pH. Therefore, **TCF-ALP** can be used to selectively detect ALP/ACP in clinical assays, or live cell systems (provided the buffer solution is optimal for the phosphatase under study).

2.3 Imaging of ALP in living cells

Prior to exploring whether **TCF-ALP** could be used to image ALP activity levels in live cells, the cytotoxicity of **TCF-ALP** was assessed using a MTT assay (**Figure S23**). Negligible cell toxicity was observed for **TCF-ALP** concentrations between 0 – 5 μM , and cell viability was only slightly reduced (91%) when incubated with 10 μM **TCF-ALP**, indicating good biocompatibility.

TCF-ALP proved cell permeable to HeLa cells that express ALP and provided a clear 'turn on' response (**Figure 3**). In contrast, pre-treatment of HeLa cells with 5 mM Na_3VO_4 prior to incubation with **TCF-ALP** resulted in minimal 'turn on'. This was taken as evidence that the increase in **TCF-ALP** fluorescence levels seen for HeLa cells in the absence of Na_3VO_4 is due to ALP activity. We thus conclude **TCF-ALP** is a probe that allows for the selective cellular imaging of ALP activity.

Bone morphogenetic protein 2 (BMP-2) is capable of inducing osteoblast differentiation into a variety of cell types (Guo et al., 2014, Wang et al., 2015) *via* pathways that result in increased ALP mRNA expression, leading to increased ALP activity (Kim et al., 2004). Treatment of myogenic murine C2C12 cells with **TCF-ALP** resulted in a low fluorescence intensity (low ALP levels) being observed (**Figure 4**); however, pre-treatment of these cells with BMP-2 (300 ng/mL, 3 days) resulted in a significant increase in **TCF-ALP**-derived fluorescence intensity (high ALP levels). Once again, pre-incubation with 5 mM Na₃VO₄ led to no fluorescence response being observed in the cells treated with **TCF-ALP** (with or without BMP-2). This provided support for the notion that **TCF-ALP** is capable of imaging endogenous ALP activity induced by BMP-2.

3 Conclusions

In summary, a long wavelength TCF-based fluorescent probe (**TCF-ALP**) has been prepared with the goal of detecting ALP activity. ALP hydrolyses the phosphate group of **TCF-ALP** resulted in a significant ‘turn on’ fluorescence response (58-fold) within 15 minutes. These spectroscopic changes were accompanied by a colorimetric change from yellow to purple. This enables **TCF-ALP** to be used as a simple assay for the evaluation of ALP activity. Further analysis revealed that **TCF-ALP** could also be used as a probe for detecting ACP activity. **TCF-ALP** was shown to be cell permeable, enabling its use as a fluorescent probe for monitoring ALP levels in HeLa cells. **TCF-ALP** also proved capable of imaging endogenously stimulated ALP produced in myogenic murine C2C12 cells through the addition of bone morphogenetic protein 2. We thus suggest that **TCF-ALP** offers promise as a tool for measuring ALP and ACP activity levels in clinical assays or in live cell systems.

4 Conflict of Interest

The authors declare that the research was conducted in the absence of any commercial or financial relationships that could be construed as a potential conflict of interest.

5 Author Contributions

LG and ACS carried out synthetic and spectroscopic experiments and co-wrote the manuscript with TDJ and JLS. JEG and GTW carried out background experiments. GK carried out cellular imaging experiments. JPL carried out the ³¹P NMR titrations. J-YM and ATAJ are supervisors of LG and GTW. SDB, JY, JLS and TDJ both conceived the idea and helped with the manuscript.

6 Funding

This work was supported in part by grant MR/N0137941/1 for the GW4 BIOMED DTP, awarded to the Universities of Bath, Bristol, Cardiff and Exeter from the Medical Research Council (MRC)/UKRI. We would also like to thank the EPSRC (EP/R003939) and the University of Bath and Public Health England for funding. ACS and JLS thank The Robert A. Welch Foundation (F-0018).

7 Acknowledgments

TDJ wishes to thank the Royal Society for a Wolfson Research Merit Award. The EPSRC UK National Mass Spectrometry Facility at Swansea University is thanked for mass analyses.

8 Supplementary Material

Data supporting this study are provided as supplementary information accompanying this paper, which is available free of charge.

9 References

- Boivin, P., and Galand, C. 1986. The human red cell acid phosphatase is a phosphotyrosine protein phosphatase which dephosphorylates the membrane protein band 3. *Biochem. Biophys. Res. Commun.*, 134, 557-564.
- Bouffard, J., Kim, Y., Swager, T. M., Weissleder, R. and Hilderbrand, S. A. 2008. A highly selective fluorescent probe for thiol bioimaging. *Org. Lett.*, 10, 37-40.
- Bull, H., Murray, P. G., Thomas, D., Fraser, A. M. and Nelson, P. N. 2002. Acid phosphatases. *J. Clin. Pathol. Molecular Pathology*. 55, 65-72.
- Cao, F.-Y., Long, Y., Wang, S.-B., Li, B., Fan, J.-X., Zeng, X. and Zhang, X.-Z. 2016. Fluorescence light-up aie probe for monitoring cellular alkaline phosphatase activity and detecting osteogenic differentiation. *J. Mater. Chem. B*, 4, 4534-4541.
- Centers For Disease Control and Prevention 2012. *Alkaline Phosphatase (ALP) in Refrigerated Serum: NHANES 2011-2012*. Available: https://wwwn.cdc.gov/nchs/data/nhanes/2011-2012/labmethods/biopro_g_met_alkaline_phosphatase.pdf [Accessed 29/01/19.]
- Coleman, J. E. 1992. Structure and mechanism of alkaline phosphatase. *Annu. Rev. Biophys. Biomol. Struct.*, 21, 441-483.
- Di Lorenzo, D., Albertini, A., and Zava, D. 1991. Progesterone regulation of alkaline phosphatase in the human breast cancer cell line T47D. *Cancer research*, 51, 4470-4475.
- Fan, C., Luo, S. and Qi, H. 2016. A Ratiometric Fluorescent Probe For Alkaline Phosphatase Via Regulation Of Excited-State Intramolecular Proton Transfer. *Luminescence*, 31, 423-427.
- Garnero, P. and Delmas, P. D. 1993. Assessment of the serum levels of bone alkaline phosphatase with a new immunoradiometric assay in patients with metabolic bone disease. *J. Clin. Endocrinol. Metab.*, 77, 1046-1053.
- Gopalan, P., Katz, H. E., McGee, D. J., Erben, C., Zielinski, T., Bousquet, D., Muller, D., Grazul, J. and Olsson, Y. 2004. Star-shaped azo-based dipolar chromophores: design, synthesis, matrix compatibility, and electro-optic activity. *J. Am. Chem. Soc.*, 126, 1741-1747.
- Guo, F., Jiang, R., Xiong, Z., Xia, F., Li, M., Chen, L. and Liu, C. 2014. Irf1a constitutes a negative feedback loop with bmp2 and acts as a novel mediator in modulating osteogenic differentiation. *Cell death dis.*, 5, e1239.
- Guo, J., Gao, M., Song, Y., Lin, L., Zhao, K., Tian, T., Liu, D., Zhu, Z., and Yang, C. 2018. An allosteric-probe for detection of alkaline phosphatase activity and its application in immunoassay. *Front. Chem.*, 6, 618.
- Hu, Q., Zhou, B., Dang, P., Li, L., Kong, J. and Zhang, X. 2017. Facile colorimetric assay of alkaline phosphatase activity using fe (ii)-phenanthroline reporter. *Chim. Acta*, 950, 170-177.
- Jiang, H. and Wang, X. 2012. Alkaline phosphatase-responsive anodic electrochemiluminescence of cdse nanoparticles. *Anal. Chem.*, 84, 6986-6993.

- 200 Jin, Y., Tian, Y., Zhang, W., Jang, S.-H., Jen, A. K.-Y. and Meldrum, D. R. 2010. Tracking bacterial
201 infection of macrophages using a novel red-emission ph sensor. *Anal. Bioanal. Chem.*, 398, 1375-1384.
- 202 Julien, S. G., Dubé, N., Hardy, S. and Tremblay, M. L. 2011. Inside the human cancer tyrosine
203 phosphatome. *Nat. Rev. Cancer*, 11, 35.
- 204 Kim, Y.-J., Lee, M.-H., Wozney, J. M., Cho, J.-Y. and Ryoo, H.-M. 2004. Bone morphogenetic
205 protein-2-induced alkaline phosphatase expression is stimulated by *dlx5* and repressed by *msx2*. *J.*
206 *Biol. Chem.*
- 207 Li, H. C., Chernoff, J., Chen, L. B. and Kirschenbaum, A. 1984. A phosphotyrosyl-protein
208 phosphatase activity associated with acid phosphatase from human prostate gland. *Eur. J. Biochem.*
209 138, 45-51.
- 210 Li, Y., Li, Y., Wang, X. and Su, X. 2014. A label-free conjugated polymer-based fluorescence assay
211 for the determination of adenosine triphosphate and alkaline phosphatase. *New J. Chem.*, 38, 4574-
212 4579.
- 213 Liao, Y., Bhattacharjee, S., Firestone, K. A., Eichinger, B. E., Paranj, R., Anderson, C. A., Robinson,
214 B. H., Reid, P. J. and Dalton, L. R. 2006. Antiparallel-aligned neutral-ground-state and zwitterionic
215 chromophores as a nonlinear optical material. *J. Am. Chem. Soc.*, 128, 6847-6853.
- 216 Liu, H.-W., Hu, X.-X., Zhu, L., Li, K., Rong, Q., Yuan, L., Zhang, X.-B. and Tan, W. 2017. In vivo
217 imaging of alkaline phosphatase in tumor-bearing mouse model by a promising near-infrared
218 fluorescent probe. *Talanta*, 175, 421-426.
- 219 Lord, S. J., Conley, N. R., Lee, H.-L. D., Samuel, R., Liu, N., Twieg, R. J. and Moerner, W. 2008. A
220 photoactivatable push–pull fluorophore for single-molecule imaging in live cells. *J. Am. Chem. Soc.*,
221 130, 9204-9205
- 222 Lowe, D., John, S., Kent, K. and Rebedew, D. 2018. Alkaline phosphatase. *StatPearls*.
- 223 Makarov, D. V., Loeb, S., Getzenberg, R. H. and Partin, A. W. 2009. Biomarkers for prostate cancer.
224 *Ann. Rev. Med.*, 60, 139-151.
- 225 Millán, J. L. 2006. Alkaline phosphatases. *Purinergic signal.*, 2, 335.
- 226 Myers, J. K. and Widlanski, T. S. 1993. Mechanism-based inactivation of prostatic acid phosphatase.
227 *Science*, 262, 1451-1453.
- 228 Ooi, K., Shiraki, K., Morishita, Y. and Nobori, T. 2007. High-molecular intestinal alkaline phosphatase
229 in chronic liver diseases. *J. Clin. Lab. Anal.*, 21, 133-139.
- 230 Pandurangan, M. and Kim, D. H. 2015. ZnO nanoparticles augment ALT, AST, ALP and LDH
231 expressions in C2C12 cells. *Saudi. J. Biol. Sci.*, 22, 679-684.
- 232 Qian, Z., Chai, L., Tang, C., Huang, Y., Chen, J. and Feng, H. 2015. Carbon quantum dots-based
233 recyclable real-time fluorescence assay for alkaline phosphatase with adenosine triphosphate as
234 substrate. *Anal. Chem.*, 87, 2966-2973.
- 235 Radio, N. M., Doctor, J. S. and Witt-Enderby, P. A. 2006. Melatonin enhances alkaline phosphatase
236 activity in differentiating human adult mesenchymal stem cells grown in osteogenic medium via
237 MT2 melatonin receptors and the MEK/ERK (1/2) signaling cascade. *J. Pineal Res.*, 40, 332-342.
- 238 Ritzke, C., Stieber, P., Untch, M., Nagel, D., Eiermann, W. and Fateh-Moghadam, A. 1998. Alkaline
239 phosphatase isoenzymes in detection and follow up of breast cancer metastases. *Anticancer Res.*, 18,
240 1243-1249.

- 241 Rosen, E., Sabel, A. L., Brinton, J. T., Catanach, B., Gaudiani, J. L. and Mehler, P. S. 2016. Liver
242 dysfunction in patients with severe anorexia nervosa. *Int. J. Eat. Disord.*, 49, 151-158.
- 243 Ruan, C., Wang, W. and Gu, B. 2006. Detection of alkaline phosphatase using surface-enhanced raman
244 spectroscopy. *Anal. Chem.*, 78, 3379-3384.
- 245 Sahran, Y., Sofian, A. and Saad, A. 2018. Pre-treatment serum lactate dehydrogenase (LDH) and
246 serum alkaline phosphatase (ALP) as prognostic factors in patients with osteosarcoma. *J Cancer.*
247 *Prev. Curr. Res.*, 9, 58-63.
- 248 Saif, M. W., Alexander, D. and Wicox, C. M. 2005. Serum alkaline phosphatase level as a prognostic
249 tool in colorectal cancer: a study of 105 patients. *J. Appl. Res.*, 5, 88.
- 250 Sedgwick, A. C., Chapman, R. S. L., Gardiner, J. E., Peacock, L. R., Kim, G., Yoon, J., Bull, S. D. and
251 James, T. D. 2017a. A bodipy based hydroxylamine sensor. *Chem. Commun.*, 53, 10441-10443.
- 252 Sedgwick, A. C., Gardiner, J. E., Kim, G., Yevglevskis, M., Lloyd, M. D., Jenkins, A. T. A., Bull, S.
253 D., Yoon, J. and James, T. D. 2018a. Long-wavelength tcf-based fluorescence probes for the detection
254 and intracellular imaging of biological thiols. *Chem. Commun.*, 54, 4786-4789.
- 255 Sedgwick, A. C., Han, H. H., Gardiner, J. E., Bull, S. D., He, X. P. and James, T. D. 2017b. Long-
256 wavelength fluorescent boronate probes for the detection and intracellular imaging of peroxynitrite.
257 *Chem. Commun.*, 53, 12822-12825.
- 258 Sedgwick, A. C., Han, H. H., Gardiner, J. E., Bull, S. D., He, X. P. and James, T. D. 2018b. The
259 development of a novel and logic based fluorescence probe for the detection of peroxynitrite and gsh.
260 *Chem. Sci.*, 9, 3672-3676.
- 261 Sun, J., Yang, F., Zhao, D. and Yang, X. 2014. Highly sensitive real-time assay of inorganic
262 pyrophosphatase activity based on the fluorescent gold nanoclusters. *Anal. Chem.*, 86, 7883-7889.
- 263 Swarup, G., Cohen, S. and Garbers, D. L. 1982. Inhibition of membrane phosphotyrosyl-protein
264 phosphatase activity by vanadate. *Biochem. Biophys. Res. Commun.*, 107, 1104-1109.
- 265 Tan, Y., Zhang, L., Man, K. H., Peltier, R., Chen, G., Zhang, H., Zhou, L., Wang, F., Ho, D. and Yao,
266 S. Q. 2017. Reaction-based off-on near-infrared fluorescent probe for imaging alkaline phosphatase
267 activity in living cells and mice. *ACS Appl. Mater. Interfaces*, 9, 6796-6803.
- 268 Teng, X., Tian, M., Zhang, J., Tang, L. and Xin, J. 2018. A tcf-based colorimetric and fluorescent
269 probe for palladium detection in an aqueous solution. *Tetrahedron Lett.*
- 270 Tibi, L., Collier, A., Patrick, A., Clarke, B. and Smith, A. 1988. Plasma alkaline phosphatase
271 isoenzymes in diabetes mellitus. *Clin. Chim. Acta.*, 177, 147-155.
- 272 Wang, G., Zhang, X., Yu, B. and Ren, K. 2015. Gliotoxin potentiates osteoblast differentiation by
273 inhibiting nuclear factor-kb signaling. *Ren. Mol. Med. Rep.*, 12, 877-884.
- 274 Wu, D., Sedgwick, A. C., Gunnlaugsson, T., Akkaya, E. U., Yoon, J. and James, T. D. 2017.
275 Fluorescent chemosensors: the past, present and future. *Chem. Soc. Rev.*, 46, 7105-7123.
- 276 Wymenga, L., Boomsma, J., Groenier, K., Piers, D. and Mensink, H. 2001. Routine bone scans in
277 patients with prostate cancer related to serum prostate-specific antigen and alkaline phosphatase. *BJU*
278 *int.*, 88, 226-230.
- 279 Yang, J., Zheng, L., Wang, Y., Li, W., Zhang, J., Gu, J. and Fu, Y. 2016. Guanine-rich dna-based
280 peroxidase mimetics for colorimetric assays of alkaline phosphatase. *Biosens. Bioelectron.*, 77, 549-
281 556.

- 282 Zhang, H., Xiao, P., Wong, Y. T., Shen, W., Chhabra, M., Peltier, R., Jiang, Y., He, Y., He, J. and Tan,
 283 Y. 2017. Construction of an alkaline phosphatase-specific two-photon probe and its imaging
 284 application in living cells and tissues. *Biomaterials*, 140, 220-229.
- 285 Zhang, H., Xu, C., Liu, J., Li, X., Guo, L. and Li, X. 2015a. An enzyme-activatable probe with a self-
 286 immolative linker for rapid and sensitive alkaline phosphatase detection and cell imaging through a
 287 cascade reaction. *Chem. Commun.*, 51, 7031-7034.
- 288 Zhang, J., Chai, X., He, X.-P., Kim, H.-J., Yoon, J. and Tian, H. 2019. Fluorogenic probes for
 289 disease-relevant enzymes. *Chem. Soc. Rev.*, 48, 683-722.
- 290 Zhang, L., Hou, T., Li, H. and Li, F. 2015b. A highly sensitive homogeneous electrochemical assay
 291 for alkaline phosphatase activity based on single molecular beacon-initiated t7 exonuclease-mediated
 292 signal amplification. *Analyst*, 140, 4030-4036.
- 293 Zhao, L., Xie, S., Song, X., Wei, J., Zhang, Z. and Li, X. 2017. Ratiometric fluorescent response of
 294 electrospun fibrous strips for real-time sensing of alkaline phosphatase in serum. *Biosens. Bioelectron.*,
 295 91, 217-224.

296

297 10 Captions for Figures and Schemes

298 **Scheme 1** – A TCF-based fluorescence probe (**TCF-ALP**) for the detection of alkaline phosphatase.

299 **Scheme 2** – Synthesis of **TCF-ALP**.

300 **Figure 1** - Fluorescence spectra of **TCF-ALP** (10 μM) produced via the addition of alkaline
 301 phosphatase (ALP; 0 – 0.2 U/ mL) in 50 mM Tris-HCl buffer, pH = 9.2 at 25 $^{\circ}\text{C}$. λ_{ex} = 542-15 nm. All
 302 measurements were made 15 min after the addition of ALP.

303 **Figure 2** - Fluorescence spectra of **TCF-ALP** (10 μM) recorded in the presence of trypsin (0.8 BAEE
 304 U/ mL), porcine liver esterase, protease from *Streptomyces griseus*, proteinase K, bovine serum
 305 albumin (0.1 mg/ mL), acid phosphatase (50 mM Tris-HCl, pH = 5.0) and alkaline phosphatase (50
 306 mM Tris-HCl, pH = 9.2). All enzymes were standardised to 0.8 U/ mL in Tris-HCl buffer pH 7.1 unless
 307 otherwise stated. λ_{ex} = 542-15 nm/ λ_{em} = 606 nm. Fluorescence measurements were made 30 min after
 308 adding the enzyme in question.

309 **Figure 3** - HeLa cells incubated under the following conditions: (a) No treatment. (b) **TCF-ALP** (10
 310 μM , 30 min). (c) Pre-treated with Na_3VO_4 (5 mM, 30 min), followed by the addition of **TCF-ALP** (10
 311 μM , 30 min). (d) Pretreated with Na_3VO_4 (0.5 mM, 30 min) and **TCF-ALP** (10 μM , 30 min). Cells
 312 were washed with DPBS before their fluorescence images were acquired using a confocal microscope.
 313 Top half: fluorescence images, bottom half: fluorescence images merged with its corresponding DIC
 314 image. Ex. 559 nm/ em. 575-675 nm. Scale bar : 20 μm . DIC - differential interference contrast.

315 **Figure 4**- **TCF-ALP** in C2C12 cell. C2C12 cells were treated with 300 ng/ mL BMP-2 for 3 days and
 316 then pretreated with 5 mM levamisole for 30 min and stained with 10 μM probe for 30 min. After
 317 washing with DPBS, fluorescence images were acquired by confocal microscopy. (a) only probe, (b)
 318 levamisole + probe, (c) BMP-2 + probe (d) BMP-2 + levamisole + probe. Top : fluorescence images,
 319 bottom : merged with DIC image. Ex. 559 nm/ em. 575-675 nm. Scale bar : 20 μm . DIC - differential
 320 interference contrast.

Figure 1.TIF

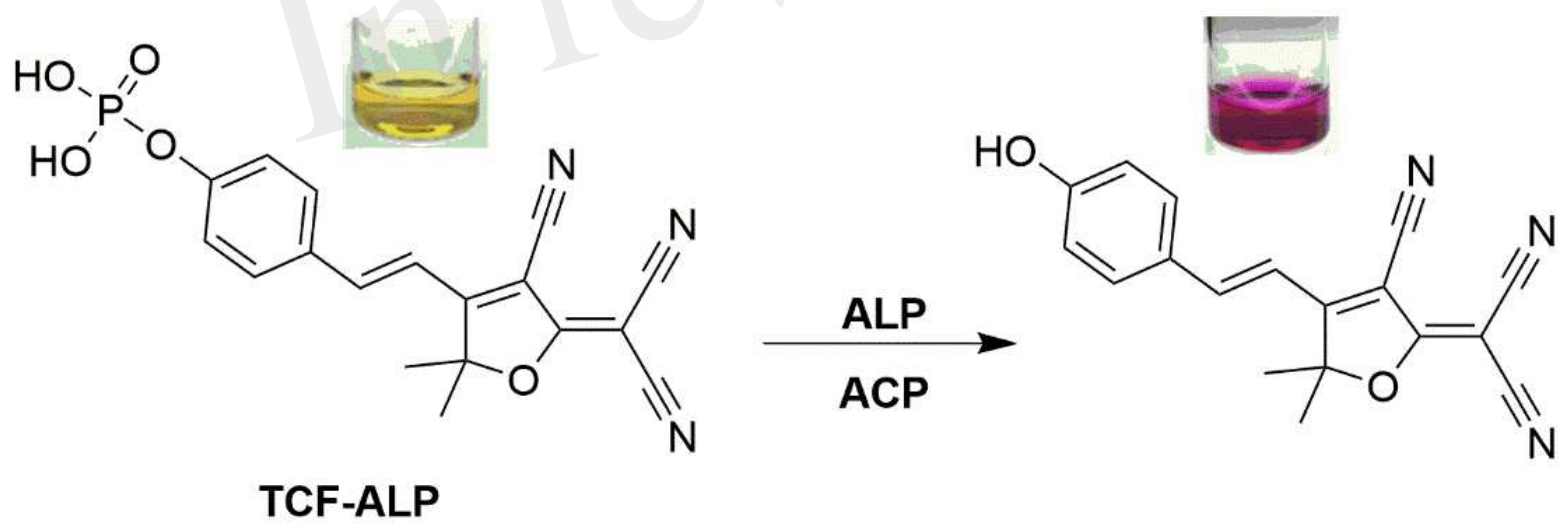


Figure 2.TIF

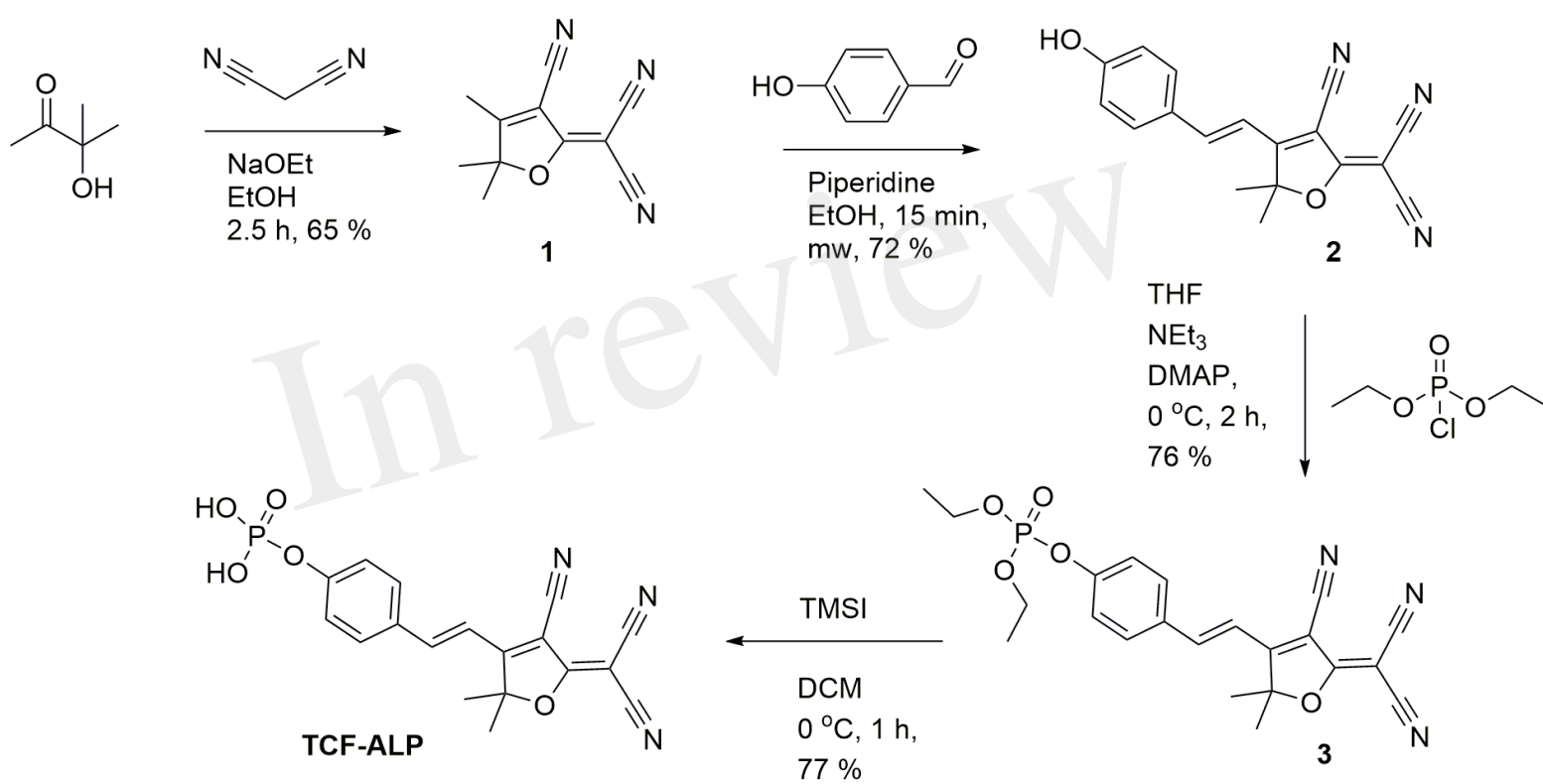


Figure 3.TIF

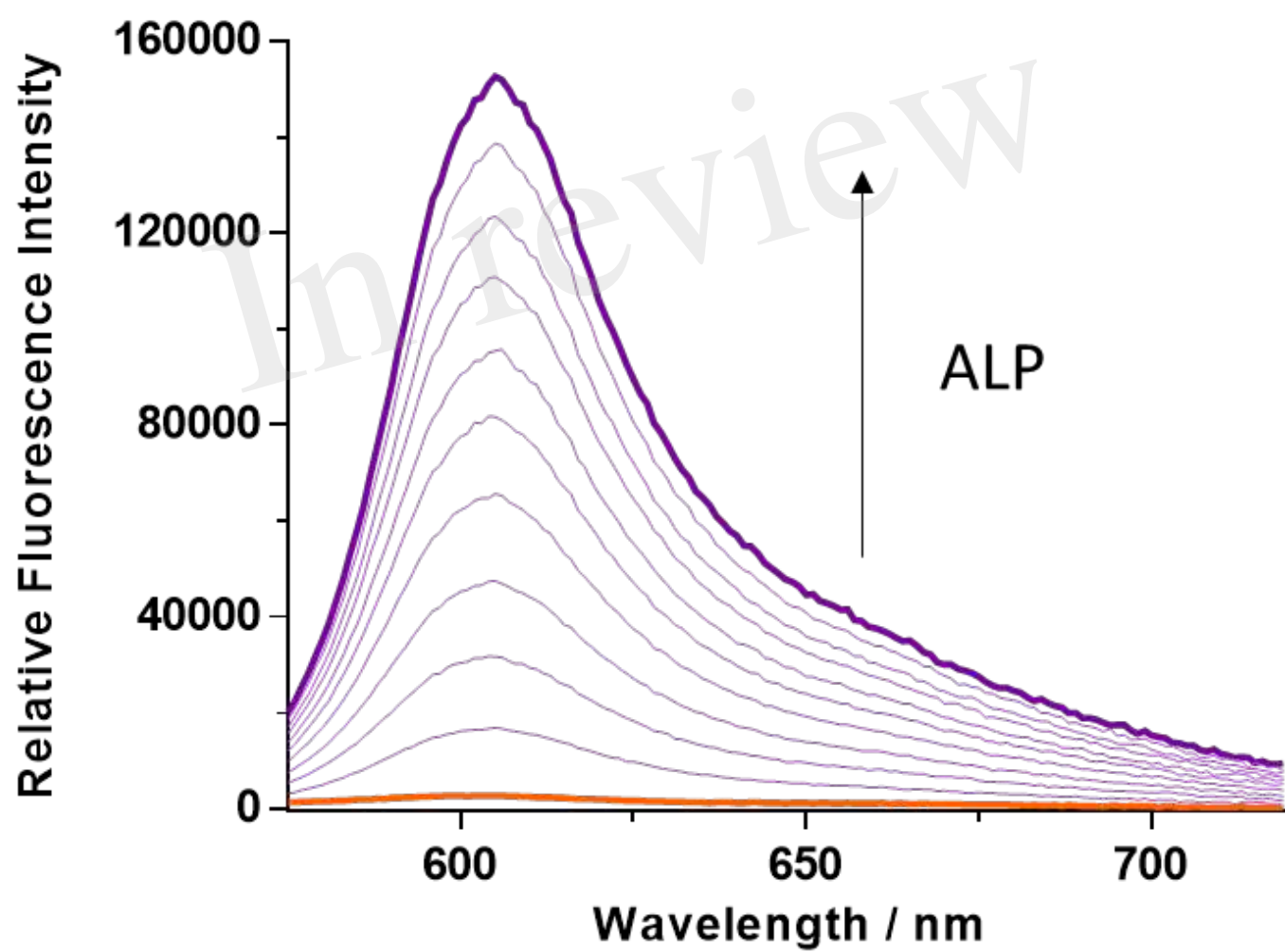


Figure 4.TIF

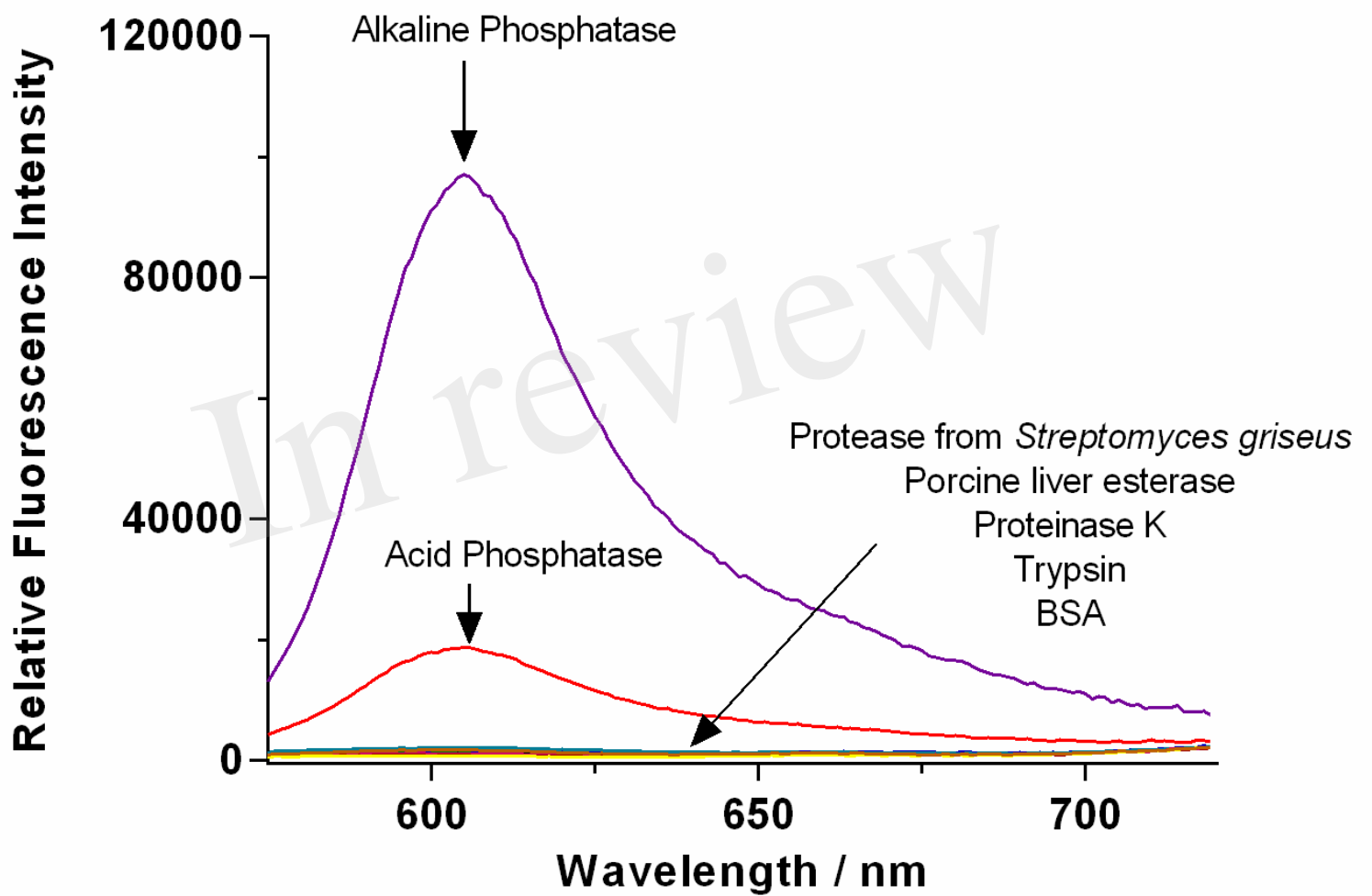


Figure 5.TIF

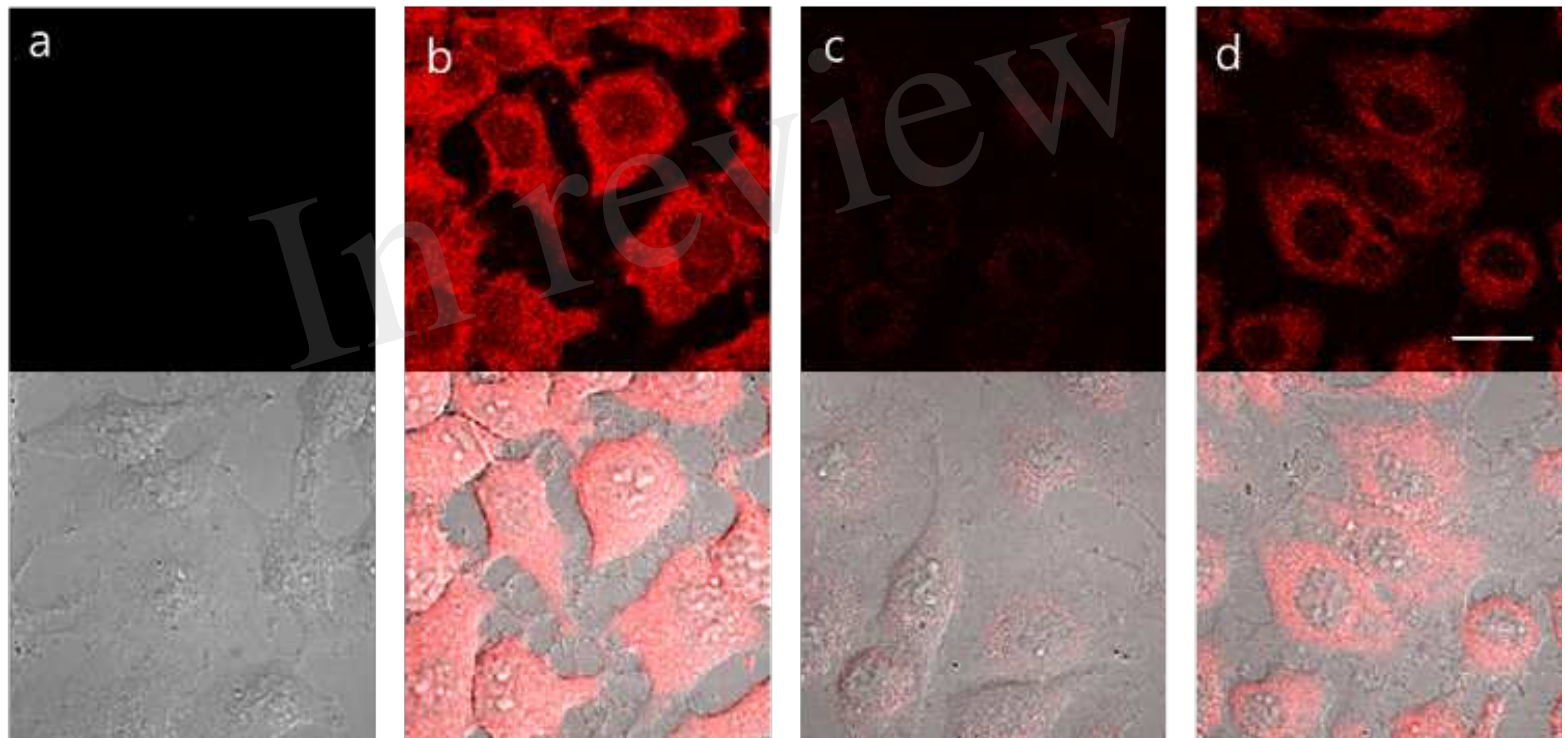


Figure 6.TIF

